AIP | Review of Scientific Instruments

High order reflectivity of highly oriented pyrolytic graphite crystals for x-ray energies up to 22 keVa)

T. Döppner, P. Neumayer, F. Girard, N. L. Kugland, O. L. Landen, C. Niemann, and S. H. Glenzer

Citation: Review of Scientific Instruments **79**, 10E311 (2008); doi: 10.1063/1.2966378
View online: http://dx.doi.org/10.1063/1.2966378
View Table of Contents: http://scitation.aip.org/content/aip/journal/rsi/79/10?ver=pdfcov
Published by the AIP Publishing

High order reflectivity of highly oriented pyrolytic graphite crystals for x-ray energies up to 22 keV[a)]

T. Döppner,[1] P. Neumayer,[1] F. Girard,[3] N. L. Kugland,[1,2] O. L. Landen,[1] C. Niemann,[1,2] and S. H. Glenzer[1]
[1]*Lawrence Livermore National Laboratory, P.O. Box 808, Livermore, California 94551, USA*
[2]*Physics Department, University of California Los Angeles, P.O. Box 951547, Los Angeles, California 90095, USA*
[3]*Commissariat à l'Énergie Atomique, Boîte Postale 12, 91680 Bruyères-le-Châtel, France*

(Presented 12 May 2008; received 12 May 2008; accepted 14 July 2008; published online 31 October 2008)

We used Kr $K\alpha$ (12.6 keV), Zr $K\alpha$ (15.7 keV), and Ag $K\alpha$ (22.2 keV) x-rays, produced by petawatt-class laser pulses, to measure the integrated crystal reflectivity R_{int} of flat highly oriented pyrolytic graphite (HOPG) up to the fifth order. The maximum R_{int} was observed in first order (3.7 mrad at 12.6 keV), decreasing by a factor of 3–5 for every successive order, and dropping by a factor of 2–2.5 at 22.2 keV. The current study indicates that HOPG crystals are suitable for measuring scattering signals from high energy x-ray sources ($E \geq 20$ keV). These energies are required to penetrate through the high density plasma conditions encountered in inertial confinement fusion capsule implosions on the National Ignition Facility. © *2008 American Institute of Physics.* [DOI: 10.1063/1.2966378]

I. INTRODUCTION

Highly oriented pyrolytic graphite (HOPG) crystals are of particular interest for x-ray diagnostics of hot dense plasmas. Their unique crystal plane structure enables them to be highly efficient x-ray diffraction instruments. These types of crystals, for example, have been successfully used in novel x-ray scattering experiments on warm dense matter[1–3] for x-ray energies of 3–9 keV. On the other hand, photon energies >10 keV are required for the probing of superdense states of matter, as encountered in inertial confinement fusion experiments.[4] The aim of this work is to characterize the reflectivity of HOPG in this energy range, i.e., between 12.6 and 22.2 keV. Since the Bragg angle decreases when going to higher photon energies, it is necessary to use the crystals in higher diffraction orders. We have characterized the performance of HOPG in up to the fifth order to ascertain their effectiveness for use in x-ray scattering experiments, especially when the detection of weak signals requires high reflectivity and good spectral resolution.

II. EXPERIMENTAL SETUP

We used the petawatt-class Titan laser facility at the Lawrence Livermore National Laboratory to produce $K\alpha$ x-rays at 12.6 keV (Kr $K\alpha$), 15.7 keV (Zr $K\alpha$), and 22.2 keV (Ag $K\alpha$). In these experiments, the Titan short-pulse laser delivered a pulse energy of up to 180 J at 1054 nm with a pulse width of 0.7 ps in the gas jet setup and 20 ps for the metal foils. A $f/3$ off-axis parabola is used to focus the beam to a $1/e^2$ spot diameter of 15 μm, yielding an intensity on target above 10^{20} W/cm^2.

To produce Zr $K\alpha$ and Ag $K\alpha$ x-rays the laser pulses were focused onto 10 μm metal foils with an incident angle of 16°. To generate Kr $K\alpha$ x-rays, the laser was interacting with a supersonic Kr gas jet.[5] We aligned the laser focus close to the gas jet nozzle and near the front edge of the gas jet in order to maximize conversion efficiency.[6] The backing pressure was kept at 90 bars to ensure the generation of large clusters and thus efficient laser absorption.[7] The neutral density of the gas jet was measured off line using a Lloyd's mirror interferometer to be 8.7×10^{19} cm$^{-3} \pm 10\%$ at the nozzle exit.

The x-ray conversion efficiency into the full solid angle was measured on each shot using a single hit counting charge coupled device[8,9] (CCD) to be $>10^{-5}$ for Kr $K\alpha$,[5] and $>10^{-4}$ for Zr $K\alpha$ and Ag $K\alpha$.[8] This technique uses a CCD camera placed far enough away from the x-ray source that a series of single photon events are recorded on the detector. Single event histogram binning[9] of the image yields an absolute number of photon events at discrete energies. In our setup, the single hit CCD observed the $K\alpha$ source from a distance of 5.4 m. Since $K\alpha$ emission is isotropic, the total number N_{total} of emitted photons can be determined.

High resolution spectra of the $K\alpha$ line emission were recorded using two HOPG spectrometers. For diffraction we used $25.4 \times 25.4 \times 2$ mm^3 ZYB grade HOPG crystals (Advanced Ceramics) with a mosaic spread of $\gamma = 0.8°$. The separation between the mosaic crystal planes is $d = 0.3354$ nm. While one spectrometer was operated in the second order for all the shots to serve as an additional source monitor, the primary instrument was used to measure the integrated HOPG reflectivity R_{int} in various diffraction orders, see Fig. 1 for the schematics of the setup. Imaging plates were used for x-ray detection. At 12.6 keV we chose plates of type Fuji BAS-SR, which previously were absolutely calibrated.[10,11] For the higher energies we utilized plates of

[a)]Contributed paper, published as part of the Proceedings of the 17th Topical Conference on High-Temperature Plasma Diagnostics, Albuquerque, New Mexico, May 2008.

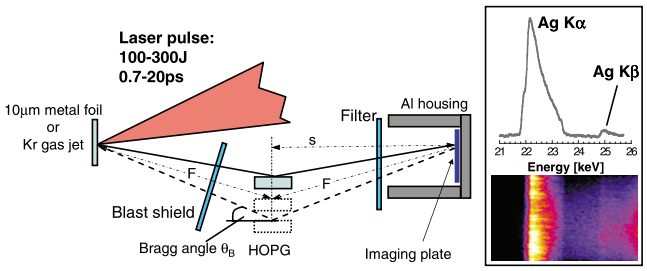

FIG. 1. (Color online) Schematics of the experimental setup used for the metal foils where $s=200$ mm was kept constant. The diffraction order was changed by adjusting the height of the HOPG crystal. For the Kr $K\alpha$ setup the focal length F (distance from source to HOPG) was fixed to 230 mm. The inset shows a raw sample image of Ag $K\alpha$ and $K\beta$ emissions recorded in the second diffraction order. As a reference for absolute reflectivity measurements a single hit CCD camera and an additional HOPG spectrometer in the second order were operated (not shown).

type Fuji BAS-MS which we measured to have a 2.8 times higher sensitivity at 22.2 keV. In the gas jet setup the spectrometer was filtered using 25 μm Mylar as blast shield and 25 μm Be plus 12 μm Al in front of the imaging plate. For Zr and Ag $K\alpha$, 25 and 400 μm Al were used as blast shield and imaging plate filter, respectively.

III. RESULTS AND DISCUSSION

For constructive interference the Bragg relationship must be satisfied: $n\lambda=2d \sin \theta_B$, where n is the diffraction order, λ is the x-ray wavelength, and θ_B is the Bragg angle. For Ag $K\alpha$ θ_B is very small for low diffraction orders (Table I), which makes it challenging to align and, in particular, for the first order, it requires very large crystals to cover the necessary bandwidth. At 12.6 keV we measured all diffraction orders from one to five. In the fifth diffraction order, the signal was below the detection threshold. At 22.2 keV the reflectivity was measured from second to fourth order. Figure 2 shows the obtained Ag $K\alpha$ line shapes. In general the measured linewidth is determined by a variety of factors, i.e., the natural linewidth, depth broadening, surface roughness, mosaicity of the crystal, and the source size, which was discussed, e.g., in Ref. 12. At higher energies in general, and at 22.2 keV in particular, the linewidth is dominated by depth broadening which is caused by reflections from lattice planes deep in the crystal. This results in a significant broadening toward the high energy side of the main line, see Fig. 2(b). Nevertheless, the instrument resolution is good enough to resolve Ag $K\alpha_1$ and Ag $K\alpha_2$. Since the attenuation length of carbon at 22.2 keV is large ($\sim$15 mm), the depth broadening

TABLE I. Bragg angles θ_B and measured integrated reflectivity R_{int} as function of diffraction order n.

n	Kr $K\alpha$ θ_B (deg)	(12.6 keV) R_{int} (mrad)	Zr $K\alpha$ θ_B (deg)	(15.7 keV) R_{int} (mrad)	Ag $K\alpha$ θ_B (deg)	(22.2 keV) R_{int} (mrad)
1	8.4	3.7	6.8		4.8	
2	17.0	1.3	13.6	0.99	9.7	0.47
3	26.1	0.21	20.7	0.21	14.6	0.12
4	35.9	0.077	28.1		19.6	0.034
5	47.1	<0.02	36.1		24.8	

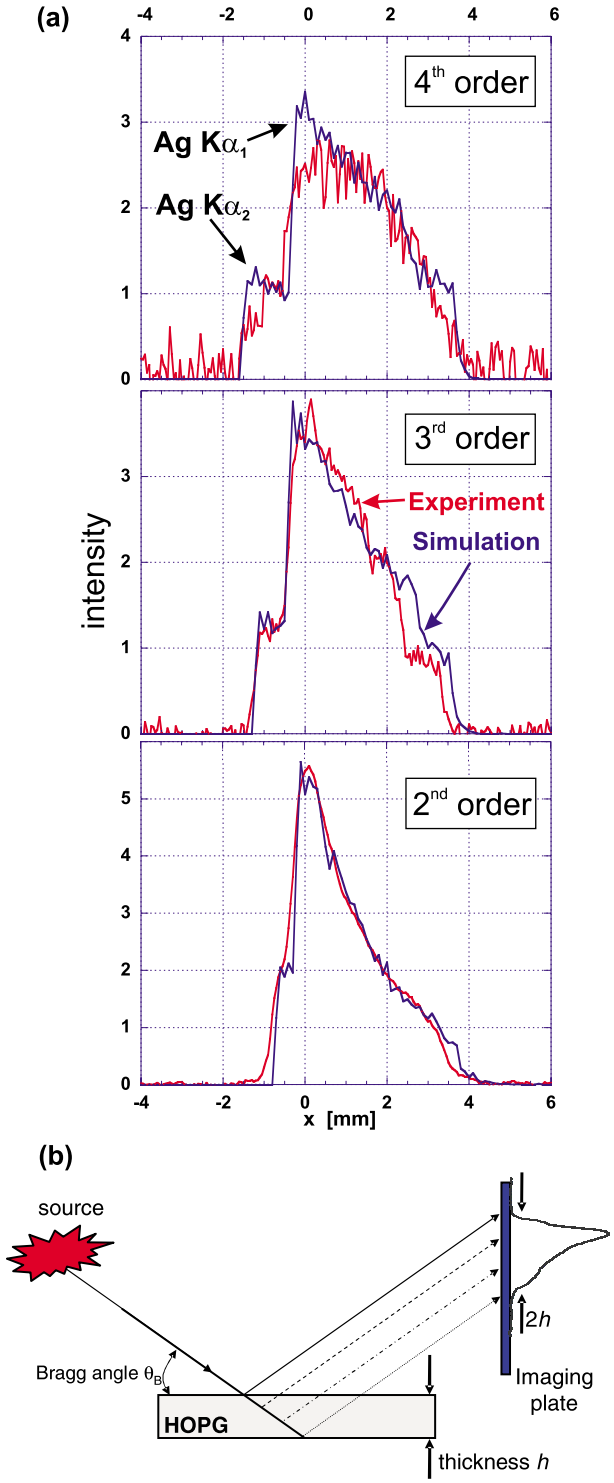

FIG. 2. (Color online) Measured Ag $K\alpha$ line shape (red) as a function of the location on the imaging plate x (a). Broadening toward higher energies is caused by reflections from deeper crystal planes and limited by the thickness $h=2$ mm of the HOPG crystal (b). The resolution of the $K\alpha_2$ (21.99 keV) and $K\alpha_1$ (22.16 keV) lines improves to higher diffraction order. The line shape is reproduced using Monte Carlo simulations (blue), for details see text.

is determined by the thickness h of the crystal. In our setup we observe a linewidth of 4 mm on the imaging plate for all diffraction orders, see Fig. 2. Note that for fixed source to detector distance $2s$ the spectral resolution due to this effect improves to higher diffraction orders as

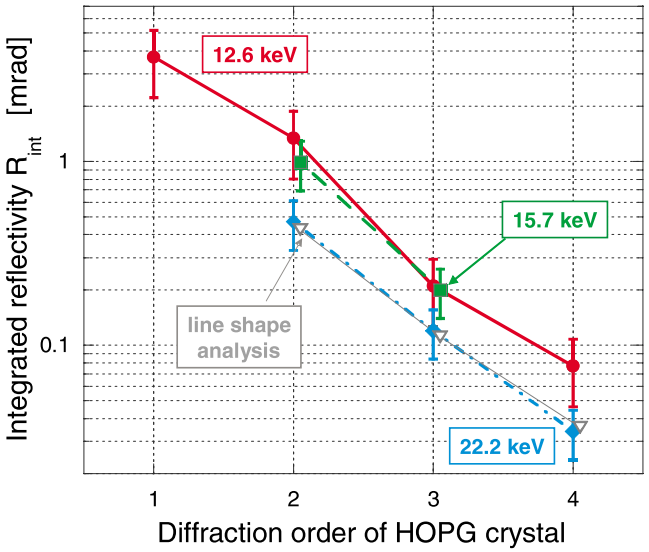

FIG. 3. (Color online) Measured integrated HOPG reflectivity R_{int} at 12.6 keV (Kr $K\alpha$), 15.7 keV (Zr $K\alpha$), and 22.2 keV (Ag $K\alpha$) up to the fourth order. For 12.6 keV the setup in the fifth order was tested, but the signal was below the detection threshold. At 22.2 keV R_{int} was extracted additionally by fitting synthetically generated spectra to the line shape (open triangles).

$$\frac{\Delta E}{E} = \frac{h}{s}\frac{\cos^3\theta_B(n)}{\sin\theta_B(n)}. \tag{1}$$

Hence in this energy range an improvement in resolution can be obtained by using higher diffraction order and decreasing the crystal thickness both of which, however, lead to a loss in signal strength at the detector.

To gain more insight into the measured Ag $K\alpha$ line shape, we performed Monte Carlo simulations which take into account the mosaicity of the crystal, the thickness of the crystal, the Bragg angle, the attenuation length in graphite, and the reflectivity R per unit length. R is adjusted to fit the simulated line shape to the measured profile. In second diffraction order R is high enough to cause a significant depletion of the x-ray pulse propagating through the crystal, i.e., the probability to observe reflections from deeper lattice planes is lower than from the surface layer.

The extracted integrated reflectivity $R_{\mathrm{int}}^{(n)}$ from these simulations are in good agreement with the values calculated from the measured signal *strength* on the detector, see Fig. 3. Hence at high x-ray energies where the linewidth is dominated by depth broadening the measurement of the line *shape* is a viable way to determine $R_{\mathrm{int}}^{(n)}$.

To obtain $R_{\mathrm{int}}^{(n)}$ from the experimental spectra, we use

$$R_{\mathrm{int}} = \frac{N_{\mathrm{IP}}}{N_{\mathrm{total}}}\frac{4\pi 2F}{\Delta x_{\mathrm{pixel}}}, \tag{2}$$

where N_{total} is the total number of $K\alpha$ photons emitted, N_{IP} is the number photons detected in a single row of pixels taking into account the filter transmission and the sensitivity of the imaging plate, $\Delta x_{\mathrm{pixel}}$ is the pixel size, and F is the distance between the source and the HOPG crystal. The spectra were typically averaged over 200 rows of 50 μm pixels. The results are shown in Fig. 3. Error bars are estimated to be 30% for the metal foils and 40% for the Kr $K\alpha$ setup. The larger error is due to the lower number of $K\alpha$ photons produced in the gas jet. In general, the signal strength decreases toward higher diffraction orders by a factor of 3–5 for every successive order. Note that, in particular for the metal foils, the ratio $R_{\mathrm{int}}^{(n)}/R_{\mathrm{int}}^{(n+1)}$ is determined with much higher precision of $\leq 5\%$. The small differences in Bragg angle make it possible to measure two diffraction orders simultaneously on the same imaging plate using two appropriately displaced HOPG crystals, see Fig. 1.

The highest reflectivity is observed at 12.6 keV in first order with 3.7 mrad. This value agrees with previous measurements at ~5 and ~8 keV.[12] At 22.2 keV R_{int} has dropped by a factor of 2–2.5 compared to the 12.6–15.7 keV range. Nevertheless, the integrated reflectivity is still up to a factor of 5 times higher than for commonly used less mosaic crystals such as LiF or PET (Ref. 13) making them suited for the detection of weak signals, as required in x-ray Thomson/Compton scattering experiments to probe dense and warm states of matter.

ACKNOWLEDGMENTS

We would like to thank the staff of the Jupiter Laser Facility for their support. This work was performed under the auspices of the U.S. Department of Energy by the Lawrence Livermore National Laboratory, through the Institute for Laser Science and Applications, under Contract No. DE-AC52-07NA27344. The authors also acknowledge support from the Laboratory Directed Research and Development under Grant Nos. 08-LW-004 and 08-ERI-002.

[1] S. H. Glenzer, G. Gregori, R. W. Lee *et al.*, Phys. Rev. Lett. **90**, 175002 (2003).
[2] G. Gregori, S. H. Glenzer, H. K. Chung, D. H. Froula, R. W. Lee, N. B. Meezan, J. D. Moody, C. Niemann, O. L. Landen, B. Holst, R. Redmer, S. P. Regan, and S. Sawada, J. Quant. Spectrosc. Radiat. Transf. **99**, 225 (2006).
[3] S. H. Glenzer, O. L. Landen, P. Neumayer, R. W. Lee, K. Widmann, S. W. Pollaine, R. J. Wallace, G. Gregori, A. Höll, T. Bornath, R. Thiele, V. Schwarz, W. D. Kraeft, and R. Redmer, Phys. Rev. Lett. **98**, 065002 (2007).
[4] J. D. Lindl, P. Amendt, R. L. Berger, S. G. Glendinning, S. H. Glenzer, S. W. Han, R. L. Kaufman, O. L. Landen, and L. J. Suter, Phys. Plasmas **11**, 339 (2004).
[5] N. L. Kugland, C. G. Constantin, C. Niemann, P. Neumayer, H. K. Chung, T. Döppner, A. Kemp, S. H. Glenzer, and F. Girard, Rev. Sci. Instrum. **79**, 10E917 (2008).
[6] N. L. Kugland, C. G. Constantin, P. Neumayer, H. K. Chung, A. , Collette, E. L. Dewald, D. H. Froula, S. H. Glenzer, A. Kemp, A. L. Kritcher, J. S. Ross, and C. Niemann, Appl. Phys. Lett. **92**, 241504 (2008).
[7] T. Ditmire, R. A. Smith, J. W. G. Tisch, and M. H. R. Hutchinson, Phys. Rev. Lett. **78**, 3121 (1997).
[8] H. S. Park, D. M. Chambers, H. K. Chung, R. J. Clarke, R. Eagleton, E. Giraldez, T. Goldsack, R. Heathcote, N. Izumi, M. H. Key *et al.*, Phys. Plasmas **13**, 056309 (2006).
[9] B. R. Maddox, H. S. Park, B. A. Remington, and M. McKernan, Rev. Sci. Instrum. 79, 10E924 (2008).
[10] N. Izumi, R. Snavely, G. Gregori, J. A. Koch, H. S. Park, and B. A. Remington. Rev. Sci. Instrum. **77**, 10E325 (2006); N. Izumi (private communication).
[11] A. L. Meadowcroft, C. D. Bentley, and E. N. Stott, "Evaluation of the sensitivity and fading characteristics of an image plate system for x-ray diagnostics," Rev. Sci. Instrum. (to be published).
[12] A. Pak, G. Gregori, J. Knight, K. Campbell, D. Price, B. Hammel, O. L. Landen, and S. H. Glenzer, Rev. Sci. Instrum. **75**, 3747 (2004).
[13] F. J. Marshall and J. A. Oertel, Rev. Sci. Instrum. **68**, 735 (1997).